

Doubly Fed Induction Generator-Based Wind Turbine Modelling and Simulation Using MATLAB/Simulink

Mohamed Gad EL-Moula Abd-Rabou^{1*}, Fathy Abd El-Lateif Elmisery², Asmaa Salah Farag Saad³,
Saber. M. Saleh⁴

¹Post Graduate Student, Electrical Engineering Dept., Faculty of Engineering, Fayoum University, Egypt

² Doctor, Electrical Engineering Dept., Faculty of Engineering, Beni-Suef University, Egypt

³ Doctor, Electrical Engineering Dept., Faculty of Engineering, Fayoum University, Egypt

⁴Associate Professor, Electrical Engineering Dept., Faculty of Engineering, Fayoum University, Egypt

Abstract - The generator acts as the primary component in a wind turbine (WT) system since it transforms mechanical energy into electrical energy. Most wind turbine malfunctions are caused by an unreliable generator. As a result, it is now more important than ever to understand the specific characteristics of the generator in wind turbines in order to avoid errors. The objective of this paper is to create a mathematical model of a wind turbine generator that is simply changeable to apply any generator fault for the research of the dynamic WT system. This is because the majority of developed WT models are either too simplistic in generator modelling or have intellectual property protection. MATLAB/Simulink was used in this research to create the mathematical model of the induction generator based on a wind turbine. The wind turbine model that was built comprises of an induction generator model, an aerodynamic model, and a wind turbine drive train based on two mass models. Electrical equations in Park's reference frame served as the basis for the development of the induction generator. Electrical and mechanical subsystems make up the model. The proposed model of the wind turbine with an induction generator was then verified using a thorough MATLAB model of a wind farm with a doubly-fed induction generator (DFIG). Comparisons were made between the two models' simulated responses for mechanical torque, electrical torque, generator speed, and power. The outcome demonstrates that both WT models' simulated responses shared the same waveform shape and dynamic behavior due to variable configuration or rating.

Key Words: Wind turbine (WT), Doubly-fed induction generator (DFIG), Wind Energy Conversion Systems (WECS), Renewable energy sources (RESSs), Synchronous rotating reference frame, Matlab / Simulink.

1. INTRODUCTION

The need for the generation of renewable energy is increasing in recent years due to social and environmental reasons, such as climate change and the dangers of fossil fuels. Given this increase in demand, a number of nations, including China, the USA, and Europe, have demonstrated the efficiency and cleanliness of producing electricity from wind turbine systems [1]. Globally, the advancement of renewable energy in contemporary production power systems has multiplied due to the rise in atmospheric

concentrations of greenhouse gases, which are incredibly harmful to our planet. When compared to other sustainable power sources, wind energy has emerged as a viable solution for generating clean energy and is now the source that is developing the fastest. However, the usage of the energy that is available is dependent on the weather (wind speed), and its integration results in volatility in the power system. The generation of power and the reduction of CO2 could change as a result of the integration of renewable energies with network connectivity, intelligent control, and storage systems. The worldwide energy storage has previously conducted an analysis of the need for a 100% renewable electricity supply [2,3]. The author of International Electrotechnical Commission claims that advances in smart grids and rising use of renewable energy are to blame for the demand for energy storage [4]. Renewable energy sources (REs) are predicted to be able to supply 70% of the world's energy requirements by 2050. The most significant energy sources will be wind, solar, and storage technologies. The utilisation of these alternative energy sources reduces dependence on fossil fuels and greenhouse gas emissions in the electrical industry [5]. The majority of nuclear and fossil fuel sources will also be totally replaced, with wind energy likely being the most prevalent and the first viable power of a worldwide energy system. Numerous academics are currently interested in initiatives to increase and improve the wind sector's participation in the power generation industry [6]. A squirrel-cage induction generator (SCIG), a doubly fed induction generator (DFIG), and a direct-drive synchronous generator (DDSG) are a few examples of the several types of generators utilised in the wind power industries [7-9]. The advantages of DFIG include its ability to independently manage active and reactive power output, a tiny power converter rated at 30% of the generator to handle the rotor power for excitation, and the capacity to control terminal voltage via reactive power control. The main cause of problems in WT is faulty generators. The generator, which is a key element in a wind turbine and is responsible for converting the mechanical energy of the wind into electrical energy, is the heart of the wind turbine. The costs of operation and maintenance will rise as a result of the rapid breakdown in WT. Therefore, a fault investigation of the generator model in the wind turbine is required to learn the specific characteristics in order to avoid the generator from breaking. The majority of WT

models are either too simplistic in their generator modelling or include intellectual property protection. Therefore, it is challenging to apply any generator flaws for the aim of WT dynamic study. In order to examine faults, a mathematical model of the induction generator in the wind turbine was created in this research. The model was subsequently confirmed using the thorough MATLAB software model of the doubly-fed induction generator (DFIG) WT.

2. The wind power system

The mechanical power generated by a wind turbine is determined by aerodynamics, and [10, 11]:

$$P_m = \frac{1}{2} \rho A C_p(\lambda, \beta) v_w^3 \quad (1)$$

Where ρ is the air density (kg/m³), is the wind speed (m/s), ($A = \pi R^2$) is swept area covered by the rotor (m²), and C_p is the power coefficient which is a function of both tip speed ratio, λ , and blade pitch angle β (deg). The efficiency of the wind turbine blades' power coefficient C_p can be analytically estimated as [16]:

$$C_p(\lambda, \beta) = 0.517 - \left(\frac{116}{\lambda_i} - 0.4\beta - 5 \right) e^{-\frac{21}{\lambda_i}} + 0.0068\lambda \quad (2)$$

$$\text{and, } \frac{1}{\lambda_i} = \frac{1}{\lambda + 0.08\beta} - \frac{0.035}{\beta^3 + 1} \quad (3)$$

The expressions in Eqs. (2) and (3) show that C_p depends on the blade pitch angle β , and the tip speed ratio λ , which is defined as:

$$\lambda = \frac{\omega_t R}{V_{wind}} \quad (4)$$

Where ω_t the angular velocity of wind turbine and R is blade radius. The turbine power characteristics are illustrated as shown in Figure 2. The pitch angle of 0° is used in this study because it results in the highest power coefficient.

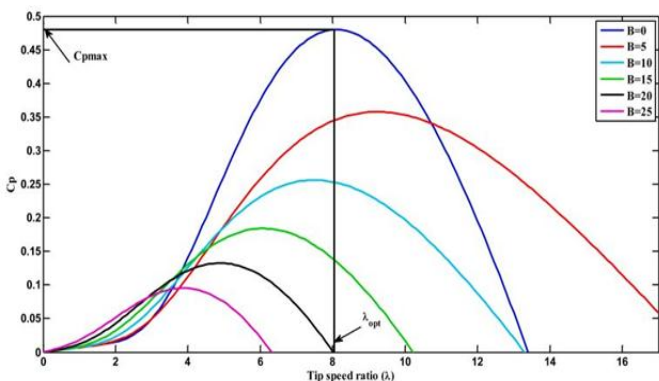


Fig -1: shows the relation between C_p and λ for different pitch angles. The maximum value of the power coefficient, $C_{pmax} \approx 0.48$, is obtained at $\beta = 0^\circ$ and $\lambda = \lambda_{opt} \approx 8.1$.

The torque produced by the wind turbine T_m is given by the following equation [12]:

$$T_m = \frac{P_m}{\omega_t} = \frac{\rho \pi R^3 v_w^2 C_p(\lambda, \beta)}{2} \quad (5)$$

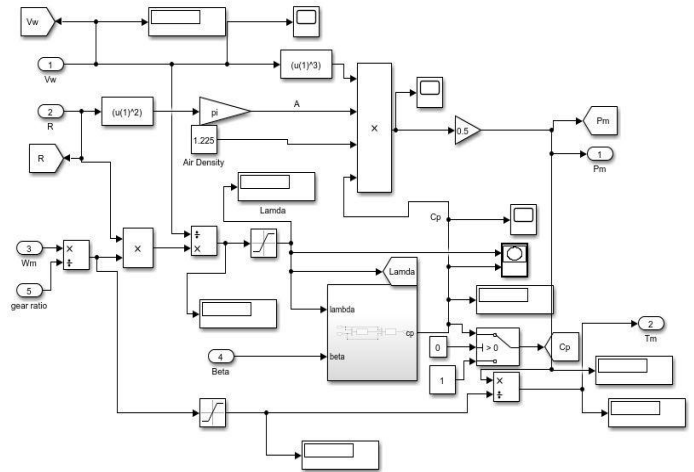


Fig -2: Simulink model of wind turbine

2.1 Mechanical drive train model

The dynamics of a wind turbine are frequently represented using a two-mass model, as in [13]. What distinguishes the two-mass model of the wind turbine from other models is the benefit of its controllers' universal design, which can be applied in wind turbines of various sizes. The two-mass model incorporates the wind turbine's adaptability as long as the modes are present [14]. Equation (6) gives the mechanical model of a two-mass wind turbine.

$$\frac{d}{dt} \omega = \frac{p}{2J} (T_m - T_s - C_f \omega) \quad (6)$$

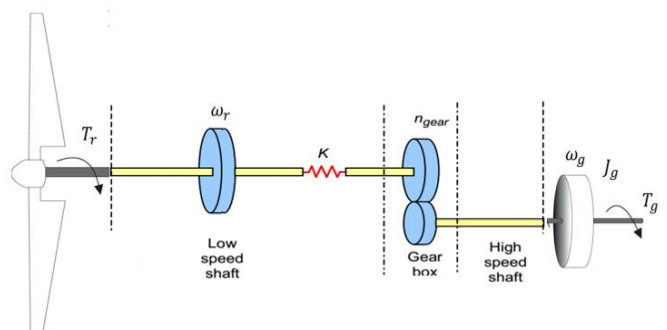


Fig -3: Configuration of drive Train With wind turbine

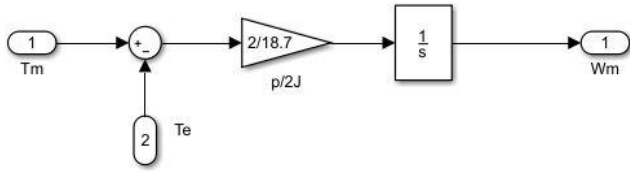


Fig -4: Simulink model of Drive Train

Where ω is the mechanical speed of the shaft, P is the number of poles of the machine, C_f is the friction coefficient, J is the inertia of the rotor, T_m is the mechanical torque generated by wind turbine, and T_e is the electromagnetic torque generated by the machine. Two-mass drive-train model is used for the simulation study in this paper.

2.2 Modelling of DFIG

The DFIG is composed of the up of the rotor and stator windings. Slip rings are present. The three-phase covered windings of the stator are connected to the grid by a three-phase transformer. The rotor consists of three-phase insulated windings, just like the stator. Slip rings and brushes are used to connect the rotor windings to an external fixed circuit, allowing the control rotor current to be injected into or removed from the windings [15–18]. Following assumptions form the basis of the DFIG model. Figure 5. Below shows the DFIG's stator can's steady state equivalent electric circuit.

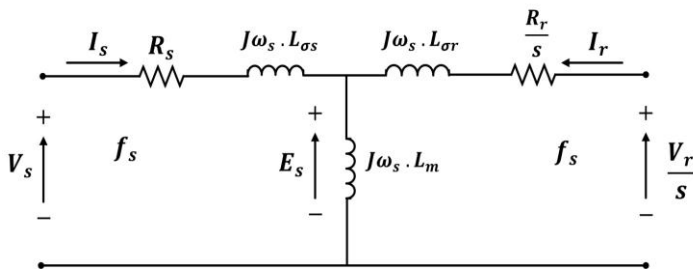


Fig -5: Equivalent circuit of the DFIG referred to stator.

The equations are calculated using direct (d) and quadrature (q) axis representation in the synchronous reference frame. The stator and rotor voltages are given by:

$$V_{ds} = R_s I_{ds} + \frac{d\lambda_{ds}}{dt} - \lambda_{qs} \omega_s \tag{7}$$

$$V_{qs} = R_s I_{qs} + \frac{d\lambda_{qs}}{dt} + \lambda_{ds} \omega_s \tag{8}$$

$$V_{dr} = R_r I_{dr} + \frac{d\lambda_{dr}}{dt} - \lambda_{qr} \omega_r \tag{9}$$

$$V_{qr} = R_r I_{qr} + \frac{d\lambda_{qr}}{dt} + \lambda_{dr} \omega_r \tag{10}$$

Where V_{ds}, V_{qs}, V_{dr} , and V_{qr} : stator and rotor voltages in the dq frame, respectively. I_{ds}, I_{qs} , and I_{qr} : stator and rotor current in the dq frame, respectively. R_s, R_r, ω_s and ω_r : stator and rotor phase resistances and angular velocity, respectively.

Where is the flux linkages are given by the expressions:

$$\lambda_{ds} = L_s I_{ds} + L_m I_{dr} \tag{11}$$

$$\lambda_{qs} = L_s I_{qs} + L_m I_{qr} \tag{12}$$

$$\lambda_{dr} = L_r I_{dr} + L_m I_{ds} \tag{13}$$

$$\lambda_{qr} = L_r I_{qr} + L_m I_{qs} \tag{14}$$

Where $\lambda_{ds}, \lambda_{qs}$ are the fluxes along the dq axis stator. $\lambda_{dr}, \lambda_{qr}$ are the fluxes along with the dq axis rotor. L_s, L_r are stator and rotor phase leakage inductances, respectively, L_m is stator-rotor mutual inductance.

$$L_s = L_{\sigma s} + L_m \tag{15}$$

$$L_r = L_{\sigma r} + L_m \tag{16}$$

Where $L_{\sigma s}$ and $L_{\sigma r}$ are the self-inductances of the stator and the rotor respectively.

The developed electromagnetic torque is given by:

$$T_e = \frac{3}{2} (\lambda_{qs} I_{dr} - \lambda_{ds} I_{qr}) \tag{17}$$

A decoupled control of the active and reactive power by the stator flux orientation to obtain separate control of the powers generated by the wind system. Controlling the dq-axes rotor currents of the DFIG will also allow for control of the stator reactive power and electromagnetic torque. The stator field revolves continuously at synchronous speed. The stator flux vector, which depicts the phase and amplitude of the flux, serves as the field symbol. Selecting the two-phase dq and placing the stator flux vector on the d-axis will allow it to write the two-phase dq related to the rotating stator field.

$$\lambda_{qs} = 0 \tag{18}$$

$$\lambda_{ds} = \lambda_s \tag{19}$$

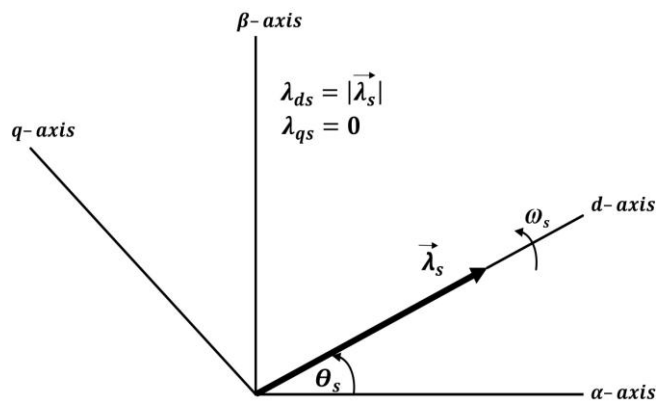


Fig -6: d-axes aligned with the stator flux space vector.

$$V_{ds} = 0 \tag{20}$$

$$V_{qs} = V_s = \lambda_s \omega_s \tag{21}$$

$$\lambda_s = L_s I_{ds} + L_m I_{dr} \tag{22}$$

$$0 = L_s I_{qs} + L_m I_{qr} \tag{23}$$

$$\lambda_{dr} = L_r I_{dr} + L_m I_{ds} \tag{24}$$

$$\lambda_{qr} = L_r I_{qr} + L_m I_{qs} \tag{25}$$

3. SIMULATION RESULTS

The simulations are executed out using MATLAB/Simulink software. In order to validate the modeling of DFIG indicated in this research, the operating point where the wind speed is constant is at 12 m/s. The DFIG and wind turbine characteristics for this simulation are reported in (Tables 1 and 2).

Table -1: The Parameters of the two-mass wind turbine mathematical model

Parameters	Constant value
Rated wind speed	12 m/s
Rated capacity	1.5 MW
Rotor radius	30.66 m
Gearbox ratio	71.28
Turbine side inertia	18.7 kg.m ²
Air density	1.225 kg/m ³
No of poles	4

Table -2: The Parameters OF DFIG

Parameters	Constant Value
Rated Voltage (line to line)	690 V
Stator resistance	2.3 m Ω
Rotor resistance	2 m Ω
Stator inductance	2.93 mH
Rotor referred inductance	2.97 mH
Mutual inductance	2.88 mH
Base Frequency	60 Hz
dc-link Voltage	937 V
dc-link capacitor	60 mF

MATLAB / SIMULINK software has been used to design and simulate the modeling of wind turbine model based on DFIG with a power of 1.5 MW.

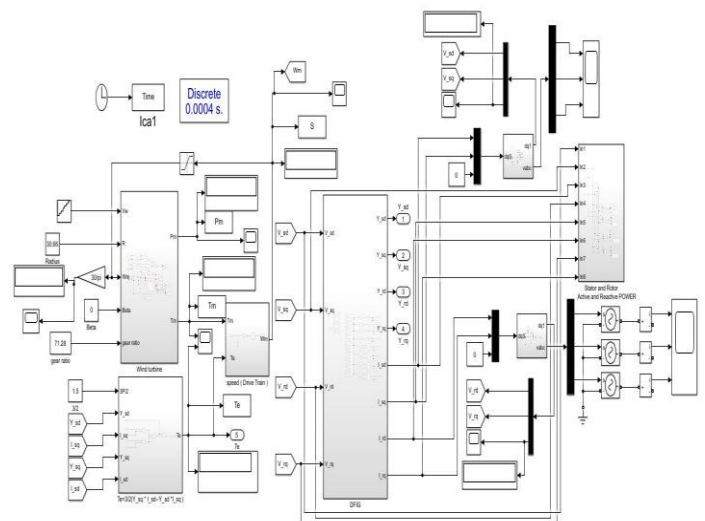


Fig.8 Overall Simulink model of wind turbine with DFIG.

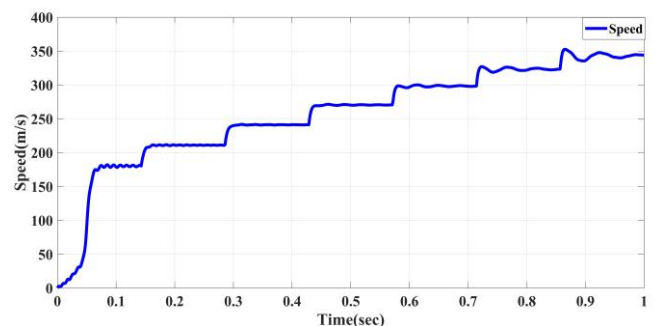


Chart -1: Response of the turbine to changes in wind speed

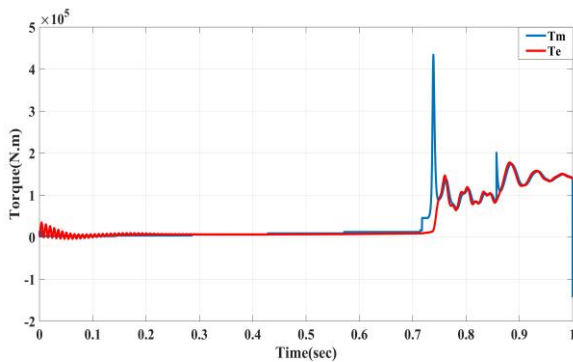


Chart -2: Electrical and Mechanical Torque.

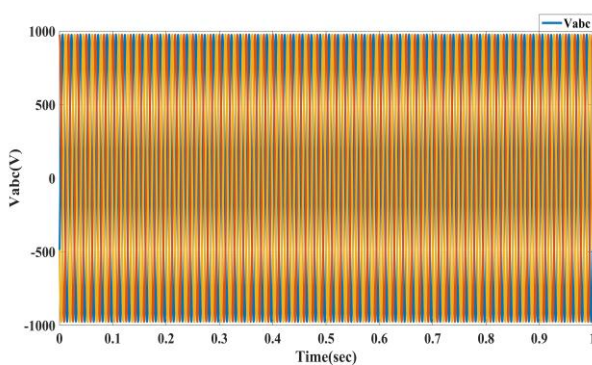


Chart -3: DFIG AC Voltage Vabc.

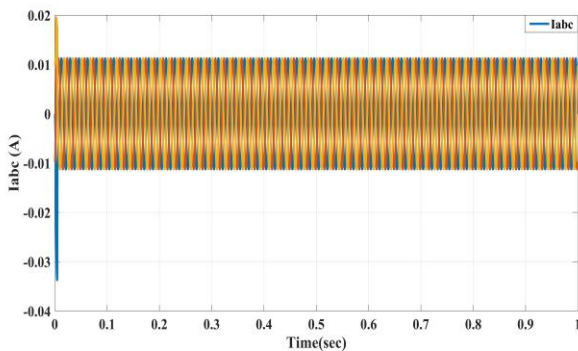


Chart -4: DFIG AC Current Iabc.

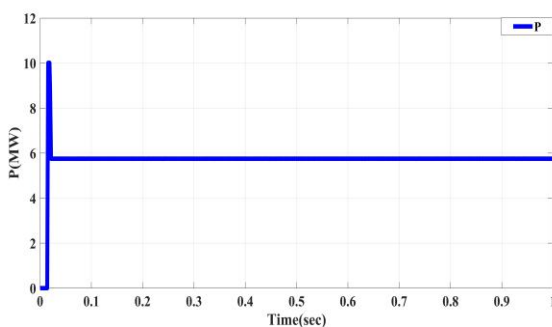


Chart -5: Mechanical Power Response.

4. CONCLUSIONS

In order to evaluate the responses and ensure the electrical distribution with the wind in terms of grid voltage and frequency fluctuations, the DFIG and dynamics operation were modelled in this study. Additionally, the primary goal of this essay is to investigate the usefulness and optimum performance of the DFIG characteristic analysis in determining the effects of a wind farm's numerous wind turbines on output variables. In order to avoid these situations and others involving fluctuation, the continuation of the research's proposal calls for the creation of a hybrid system made up of multiple wind turbines and an energy storage system. This hybrid system will give a precise idea of the distribution and level of fluctuations as presented in the analysis and simulation in the pitch angle, current, and voltage curves. Non-isolated power converters will be used to regulate each subsystem, and the inverter will be used to connect them to the grid or a local load.

Energy management across all hybrid system components will enhance simulations of the intelligent control system. Therefore, it is not sufficient to say that one energy storage technology is superior to all others for each generator; rather, it is more accurate to say that each of them performs better and is more appropriate for particular applications. To overcome the drawbacks of DFIG generating wind turbines and enable the use of electronic power converters, several configurations will be researched. The storage components of the hybrid system increase its adaptability and capacity to control and regulate its active power generation in order to meet changing grid demand.

Abbreviations

The following abbreviations and notations are used in this manuscript:

<i>DFIG</i>	Doubly fed induction generator
<i>RES</i>	Renewable energy sources
<i>PWM</i>	Pulse width modulation
<i>WECS</i>	Wind energy conversion systems
ω_r	Rotational speed of turbine
V_w	Wind speed
λ	Tip speed ratio
β	Blade pitch angle
U	Voltage
R	Resistance
P_w	Power wind turbine
C_p	Polynomial function of λ and β

REFERENCES

[1] International Energy Agency. Global Energy Review. 2021. Available online: <https://www.iea.org/reports/global-energy-review-2021/renewables> (accessed on 10 January 2022).

- [2] Pleßmann, G.; Erdmann, M.; Lusaka, M.; Breyer, C. Global energy storage demand for a 100% renewable electricity supply. *Energy Procedia* 2014, 46, 22–31. 294, Dec. 2001, pp. 2127–2130, doi:10.1126/science.1065467.
- [3] Bussar, C.; Moos, M.; Alvarez, R.; Wolf, P.; Thien, T.; Chen, H.; Cai, Z.; Leuthold, M.; Sauer, D.U.; Moser, A. Optimal allocation and capacity of energy storage systems in a future European power system with 100% renewable energy generation. *Energy Procedia* **2014**, 46, 40–47.
- [4] IEC White Paper Energy Challenge:2010. *Coping with the Energy Challenge The IEC's Role from 2010 to 2030*; IEC: Geneva, Switzerland, 2010.
- [5] IRENA. *Global Energy Transformation: A Roadmap to 2050*, 2018th ed.; IRENA: Abu Dhabi, UAE, 2018.
- [6] Sun, Z.; Wang, H.; Li, Y. Modelling and simulation of doubly-fed induction wind power system based on Matlab/Simulink. *IET Conf. Publ.* 2012.
- [7] Rolán, A.; Pedra, J.; Córcoles, F. Detailed study of DFIG-based wind turbines to overcome the most severe grid faults. *Int. J. Electr. Power Energy Syst.* **2014**, 62, 868–878.
- [8] Fernández, L.M.; García, C.A.; Saenz, J.R.; Jurado, F. Equivalent models of wind farms by using aggregated wind turbines and equivalent winds. *Energy Convers. Manag.* **2009**, 50, 691–704.
- [9] Krim, Y.; Abbes, D.; Krim, S.; Mimouni, M.F. Intelligent droop control and power management of active generator for ancillary services under grid instability using fuzzy logic technology. *Control Eng. Pract.* **2018**, 81, 215–230.
- [10] Boukhezzer B, Siguerdidjane H. Nonlinear control of a variable-speed wind turbine using a two-mass model. *IEEE Trans Energy Convers* 2011; 26(1):149–62.Mar.
- [11] Ghasemi S, Tabesh A, Askari-Marnani J. Application of fractional calculus theory to robust controller design for wind turbine generators. *IEEE Trans Energy Convers* 2014; 29(3):780–7. Sep.
- [12] Liu J, Gao Y, Geng S, Wu L. Nonlinear control of variable speed wind turbines via fuzzy techniques. *IEEE Access* 2017; 5:27–34.
- [13] Novak P, Ekelund T, Jovik I, Schmidtbauer B. Modeling and control of variable-speed wind-turbine drive-system dynamics. *IEEE Control Syst* 1995;15(4):28–38.Aug.
- [14] Boukhezzer B, Siguerdidjane H, Hand MM. Nonlinear control of variable-speed wind turbines for generator torque limiting and power optimization. *J Sol Energy Eng* 2006; 128(4):516–30. Aug.
- [15] Hore, D.; Sarma, R. Neural Network-based Improved Active and Reactive Power Control of Wind-Driven Double Fed Induction Generator under Varying Operating Conditions. *Wind Eng.* 2018, 42, 381–396.
- [16] Carroll, J.; McDonald, A.; McMillan, D. Reliability Comparison of Wind Turbines with DFIG and PMG Drive Trains. *IEEE Trans. Energy Convers.* 2015, 30, 663–670.
- [17] Hosseini, S.M.H.; Rezvani, A. Modeling and Simulation to Optimize Direct Power Control of DFIG in Variable-Speed PumpedStorage Power Plant Using Teaching-learning-Based Optimization Technique. *Soft Comput.* 2020, 24, 16895–16915.
- [18] Xia, Y.; Chen, Y.; Song, Y.; Strunz, K. Multi-Scale Modeling and Simulation of DFIG-Based Wind Energy Conversion System. *IEEE Trans. Energy Convers.* 2020, 35, 560572.